

Chemical mechanical polishing: Theory and experiment

Dewen ZHAO, Xinchun LU*

State Key Laboratory of Tribology, Tsinghua University, Beijing, 100084, China

Received: 25 October 2013 / Accepted: 24 November 2013

© The author(s) 2013. This article is published with open access at Springerlink.com

Abstract: For several decades, chemical mechanical polishing (CMP) has been the most widely used planarization method in integrated circuits manufacturing. The final polishing results are affected by many factors related to the carrier structure, the polishing pad, the slurry, and the process parameters. As both chemical and mechanical actions affect the effectiveness of CMP, and these actions are themselves affected by many factors, the CMP mechanism is complex and has been a hot research area for many years. This review provides a basic description of the development, challenges, and key technologies associated with CMP. We summarize theoretical CMP models from the perspectives of kinematics, empirical, its mechanism (from the viewpoint of the atomic scale, particle scale, and wafer scale), and its chemical–mechanical synergy. Experimental approaches to the CMP mechanism of material removal and planarization are further discussed from the viewpoint of the particle wear effect, chemical–mechanical synergy, and wafer–pad interfacial interaction.

Keywords: chemical mechanical polishing (CMP); CMP model; planarization mechanism; wafer–pad interaction; uniformity

1 Introduction

The chemical mechanical polishing/planarization (CMP) process was developed at IBM and was first used in oxide polishing in 1986, and in tungsten polishing in 1988. After several decades of development, it has become accepted worldwide as a mainstream process in the fabrication of planar film. Using CMP, planar, smooth, and damage-free surface can be obtained.

By definition, CMP is a process whereby both chemical and mechanical actions complement each other to improve the material removal rate (MRR). CMP can produce both global and local planar surfaces to the wafer by micro, nano, or atomic material removal, so as to satisfy the planarity constraint imposed by current advanced lithography processes [1]. Over the past few decades, CMP has emerged as a necessary planarization process in the manufacture of integrated circuits (IC) products because of its effective performance in thinning and flattening thin films.

In chip manufacturing, the front-end process fabricates the circuit elements, while the back-end process wires these elements within an integrated circuit. Both the front-end and the back-end processes need the CMP process to produce a flat structure. To accommodate the improvements of decreased feature size and increased device speed, chip interconnects, which function as back end of the line (BEOL) processes, have become as important as the front end of the line (FEOL) processes [2, 3]. CMP is one of the most important processes in the BEOL processes [4]. Figure 1 shows the section view of Intel's 65 nm technology silicon back-end interconnect stack with 8 metal layers [5]. With CMP process, the interconnect materials can be stacked layer upon layer.

In keeping with Moore's law, the IC manufacture process has for many years seen the developing of small feature size, increased wafer size, and higher integration. Presently, 300 mm wafers are widely used, and 450 mm wafers are expected to emerge in several years, while the interconnections have exceeded 10

* Corresponding author: Xinchun LU.
E-mail: xclu@tsinghua.edu.cn

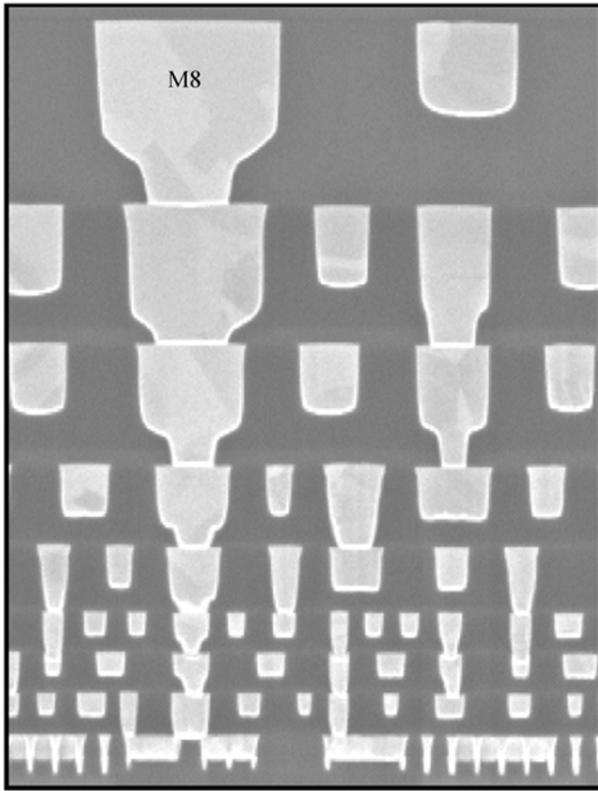


Fig. 1 Section view of Intel's 65 nm technology silicon back-end interconnect stack (adapted from Intel Developer Forum 2009 [5]).

levels. Therefore, CMP faces many challenges that need to be overcome, such as the need to provide nano level planarity and sub-nano level roughness to wafer surfaces, while avoiding surface and subsurface damage, which has almost reached the limit in surface manufacturing.

To improve the CMP technique, two aspects of the mechanism must first be investigated. On one hand, we need to understand the micro/nano/atomic scale material removal mechanism caused by the synergetic effects of chemical and mechanical actions. On the other hand, for large-dimension wafers, we need to know how to achieve a global planar surface by local material removal.

In this paper, we review the main factors, key challenges, and technologies of CMP. Theoretical models will be introduced from the viewpoint of the atomic scale, particle scale, and wafer scale. In addition, we will review experimental studies regarding its mechanism and process.

2 Basics of CMP

2.1 Principle of CMP

There are four types of commercially available CMP equipments that are most representative and most widely used in industry (see Fig. 2): (a) a rotary-type polisher with a wafer carrier that has a reciprocation motion along the platen diameter; (b) a rotary-type polisher with a carrier that has an oscillation motion; (c) an orbital-type polisher with the platen that has an orbital rotation; (d) a linear-type polisher that has a linear motion belt as the polishing pad.

For the typical rotary type CMP tool, the platen and the wafer carrier rotate in the same direction, while the wafer carrier reciprocates synchronously along the radial direction of the platen. The wafer is held in a rotating carrier, as shown in Fig. 3(a). The carrier has a membrane that applies the downforce on the wafer back, and a retaining ring around the outside of the wafer to keep the wafer in the carrier. A polishing pad is mounted on the rotating platen. The surface of the wafer being polished is pressed against the

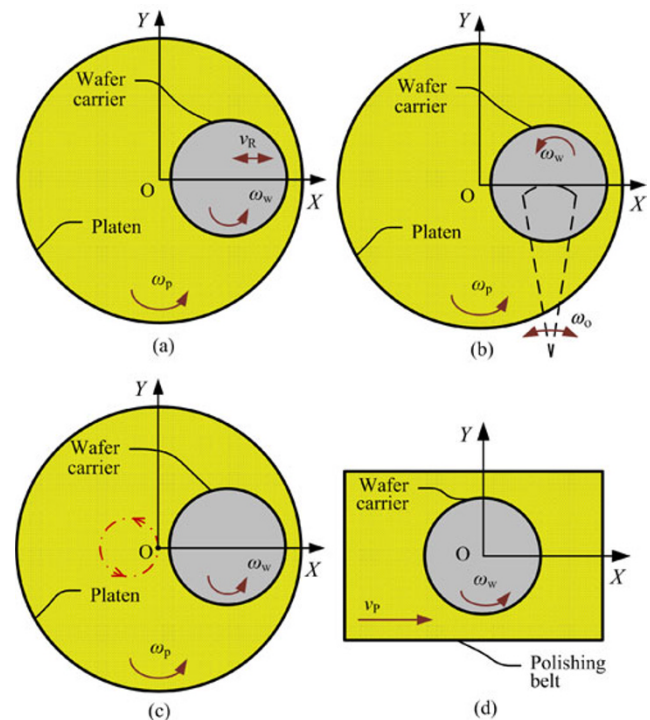


Fig. 2 Schematic of different types of CMP equipment: (a) rotary type, reciprocation mode, (b) rotary type, oscillation mode, (c) orbital type, and (d) linear type.

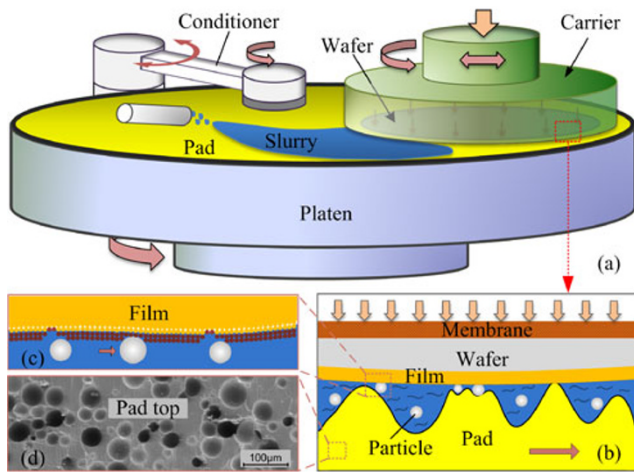


Fig. 3 Schematic of CMP equipment and wafer-pad interactions: (a) CMP equipment, (b) wafer-pad interactions, (c) details of particle-film interactions, and (d) SEM image of pad top surface.

polishing pad. The motions of the carrier and the platen generate the relative motion for the polishing. A slurry containing particles and chemical solutions is delivered on the pad as the abrasive. Figures 3(b), 3(c), and 3(d) give a detailed schematic diagram of wafer-pad interactions, particle-film interactions, and

the SEM image of the pad top surface, respectively. The chemical reaction softens the deposited film surface to enable it to be a more easily removed layer. From the combination of the chemical actions of the chemicals and the mechanical actions of the particles, micro material removal takes place, enabling surface finishing to be realized [6].

2.2 Main factors

The MRR, the non-uniformity, and the surface quality are the main results which indicate the machine’s efficiency and surface quality. Factors that are related to the wafer-pad interaction can affect the polishing results. The major factors include machine structures (e.g., carrier structure), process parameters (e.g., downforce and kinematic parameters), and consumables (e.g., slurry and pad), as shown in Fig. 4. These input variables affect the wafer pad interaction, including the pressure/stress distribution, the slurry film distribution, the sliding distance distribution, and the temperature distribution. The final polishing results are determined by the synergetic action of the above process parameters [7].

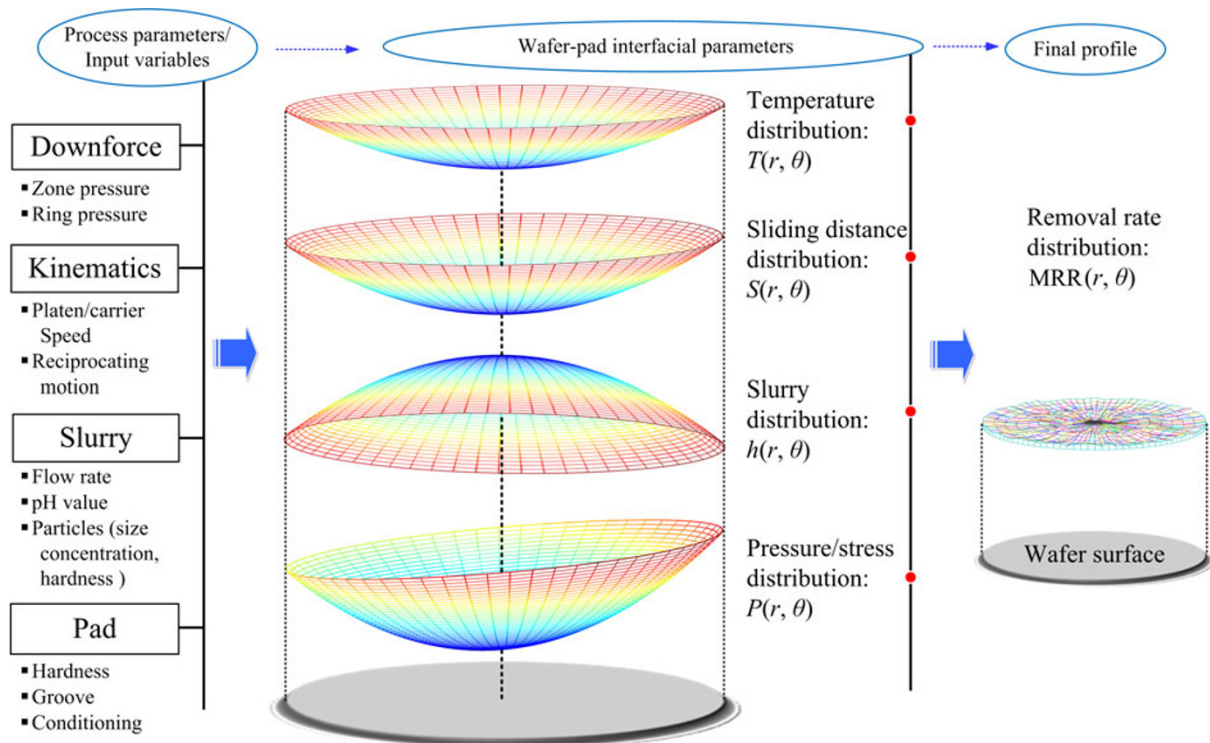


Fig. 4 Schematic of CMP factors affecting the final profile.

2.2.1 Carrier structure

Previous wafer carriers use a fixed rigid packing plate and a fixed retaining ring to grip the wafer and to apply the polishing pressure [8], as shown in Fig. 5(a). Because the ring cannot be applied to a separate pressure to accommodate the wafer contact pressure, the wafer edge has a large edge exclusion due to the edge effect. To improve the uniformity of the wafer contact stress, a flexible membrane is used to load the wafer and to apply a soft load on the wafer's back surface. In addition, a floating ring which can be separately loaded is used as the retaining ring, as shown in Fig. 5(b). The retaining ring can effectively shift the stress concentration near the wafer edge to the surface of the retaining ring. Usually, a relatively larger pressure is applied to the retaining ring to ensure that the wafer has a uniform contact stress; as a result, good uniformity and smaller edge exclusion can be realized for the wafer [9, 10].

However, when the wafer diameter increases to 300 mm or larger, a uniform load pressure cannot produce a uniform contact pressure. Besides, the wafer may have an incoming surface topography. Therefore, to improve the uniformity of the CMP for a large-size wafer, a novel multizone carrier is developed, and is widely used in today's industrialized CMP equipment, as shown schematically in Fig. 5(c). The multizone carrier has a multizone membrane for the application of individual pressures to different eccentric zones and the retaining ring [11]. Using this technique and

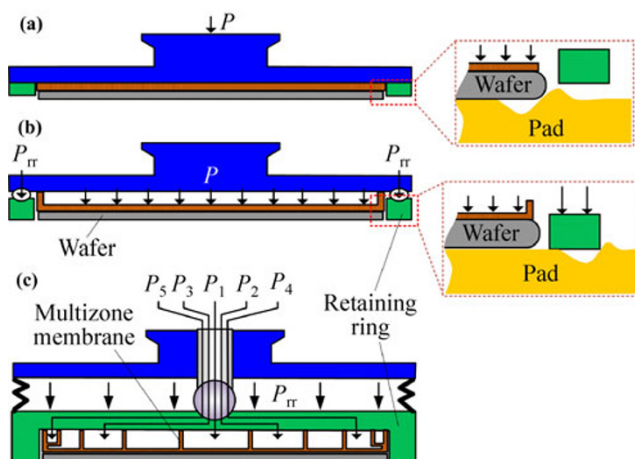


Fig. 5 Schematic section view of wafer carrier: (a) hard plate carrier with no ring pressure, (b) flexible membrane carrier with ring pressure, and (c) multizone carrier.

the corresponding process control method, a marked improvement in the global uniformity of the wafer after CMP can be realized.

2.2.2 Polishing pad

The polishing pads are usually made of porous polyurethane, with a filler material added to modify pad hardness [4]. The hardness of the pad is one of its most important properties, and can affect both the MRR and uniformity. Both the hard pad and soft pad are needed for different film materials and different process steps. Soft pads, such as Suba and Politex, and hard pads, such as IC1000 and IC1010, are most widely used in IC manufacturing. The details of pad top in Fig. 3(d) give the SEM image of an IC1000 pad. The bulk materials and the surface are full of micropores, which are useful for storing the slurry and the abrasive particles in the slurry, and they survive the aggressive slurry chemistries.

Due to mechanical loads and chemical reactions at the pad surface, physical properties of a CMP pad, such as the elastic modulus, compressibility, hardness, and surface roughness, are expected to vary during CMP [12–14]. These changes may have important effects on the overall CMP process. Therefore, a pad conditioner is used to introduce a pad conditioning process that can generate new asperities on the pad surface to maintain the pad performance (see Fig. 3(a)). With the exception of the mechanical properties of the pad, grooves on the pad comprise another important factor for the pad, and are used for slurry transfer and for removing the polishing debris. A reasonable groove design may result in good polishing results [15].

2.2.3 Slurry

Slurry is the most complex consumable of CMP. The slurry is a stable mixture of abrasive materials dispersed in DI wafer with other chemicals, such as oxidant, inhibitor, surfactant, and bases to provide an acid or alkaline pH. Particles such as SiO_2 , CeO_2 , and Al_2O_3 , with the average particle size ranging from 10 to 100 nanometers, can be used as the abrasive. The chemical elements, particles size and concentration, as well as the pH value of the solution can affect the MRR, uniformity, and surface quality. Especially, the interaction and balance of the oxidant, inhibitor, and

complexing agent can significantly affect the polishing results [16, 17].

2.2.4 Process parameters

As shown in Fig. 4, the removal rate profile is codetermined by the wafer–pad interfacial parameters of pressure distribution, sliding distance distribution, temperature distribution, and slurry distribution. Many process parameters, such as the downforce (including the zone pressure and the ring pressure), the kinematic parameters (including the carrier/platen speed and reciprocating motion parameters), the slurry (including its flow rate, pH value, and particle parameters), and the pad (including its hardness, groove form, and conditioning parameters), can affect the final polishing results by modifying above interfacial parameters at the wafer–pad interface.

2.3 Development trend and main challenges

2.3.1 Feature size and wafer dimension

With the development of different technique, integrated circuits have trended toward having smaller size, higher integration, and lower price. As a result, several new challenges have emerged for the CMP process. Base on the International Technology Roadmap for Semiconductors (ITRS 2012 [18]), both STI CMP and interconnect CMP are being developed toward sub-22 nm node (see Table 1).

The ITRS 2012 predicts that by 2015, the half pitch of Metal 1 will be below 22 nm, and will be further reduced to 14 nm by 2019. However, as the feature size decreased, the focus depth of the lithography is shortened accordingly. The nonuniformity of the wafer surface will therefore result in a nonuniform lithography width, subsequently leading to chip failure.

For the ultra-large scale integrated-circuit (ULSI), the number of transistors that are fitted on a single chip has exceeded 1 billion. Multi-lever interconnects are introduced to improve the connection efficiency. With the increasing number of transistors per chip, the number of interconnect layers also increases. For the 65 nm node, there are 9–10 layers, and when the feature size is below 45 nm, the number of interconnect layers exceeds 10, while the 32 nm node needs 12 layers,

and the 22 nm node needs 13 layers. The nonuniformity will accumulate when the number of interconnect layers increases, which may introduce additional challenges to the CMP process.

To increase the production efficiency and to reduce the chip cost, the wafer dimension has been increased from 200 mm (8 inches) to 300 mm (12 inches), and subsequently toward 450 mm. The semiconductor industry has effectively adapted its CMP technology for the 300 mm wafer. For large-diameter wafers, the realization of global planarity across the whole wafer will also be a major challenge for CMP.

2.3.2 Low-*k* material

To reduce the RC delay of the device, copper interconnects have been introduced to replace Al interconnects, and the damascene process has been introduced. Ultra low-*k* materials will be used as interlayer dielectrics to further decrease the RC delay. According to the ITRS roadmap 2012, materials with a dielectric constant of 2.2 will be integrated into the IC by the year 2019 (Table 1). However, the low-*k* dielectrics are soft and weak relative to the metal material. Both of the single and dual damascene structures comprising ultra low-*k* materials are more prone to buckling and crushing failures. The difference between the mechanical property and polishing rates of copper and the low-*k* materials will significantly

Table 1 Interconnect CMP demand from ITRS 2012 [18].

Year	Metal 1 wiring half-pitch (nm)	Number of metal levels	Interlevel metal insulator effective dielectric constant, <i>k</i>
2012	32	12	2.82–3.16
2013	27	13	2.55–3.00
2014	24	13	2.55–3.00
2015	21	13	2.55–3.00
2016	19	13	2.40–2.78
2017	17	14	2.40–2.78
2018	15	14	2.40–2.78
2019	13	14	2.15–2.46
2020	12	14	2.15–2.47
2025	7	16	1.60–2.00

affect post-CMP surface planarity and surface quality. New technologies and processes, such as stress free CMP and low downforce CMP, are therefore demanded to be developed to address these problems [19].

2.4 Key technology of CMP

2.4.1 Pressure control

As the original surface profile of wafers produced from the electrochemical plating (ECP) process is not sufficiently planar, traditional one-zone CMP cannot control the profile (especially at the wafer edge) for different incoming wafers. Thus, a new type of multizone CMP was developed, and is expected to improve the uniformity and to provide a wider processing window. Unlike the typical single-zone configuration, the wafer carrier is divided into multiple zones in the radial position, and different pressures can be applied to each zone individually (see Fig. 5(c)). Using this technique, the within-wafer nonuniformity (WIWNU) can be significantly improved.

Further, using the multizone carrier, a closed-loop zone pressure control technology was developed in AMAT's machine based on *In Situ* Profile Control (ISPC™) using next generation polishing heads. Using the real-time profile adjustments technique, the ISPC system can significantly improve the post-polish within-wafer and wafer-to-wafer non-uniformity. The zone-to-zone range was improved from 1300 Å open-loop to 70 Å with ISPC control for ILD0 CMP, and from 870 Å open-loop to 200 Å with ISPC control for STI CMP [20].

2.4.2 Endpoint detection

In-line monitoring and automatic endpoint detection of CMP can provide information regarding the film thickness, surface profile, and the time at which the film will be fully removed [21]. It offers many advantages to the manufacturing process such as improved process yields, reduced product variability, closer conformance to target requirements, and higher throughput. The optical method [22, 23], eddy current method [21], and motor current detecting [24] are most widely used as the in-line monitoring methods for the endpoint, and Fig. 6 shows the schematic configurations of these endpoint detection methods.

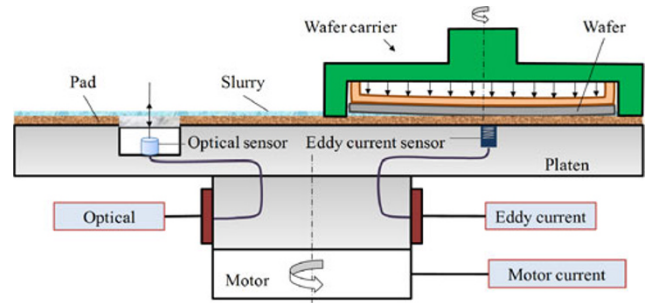


Fig. 6 Schematic of endpoint detection.

3 Kinematics and stress simulation for CMP

3.1 Kinematic simulation

The kinematic aspect is the most basic uniformity factor that affects the final polishing results [25–28]. The relative motion between the wafer and the pad is produced by the three basic motions of the carrier and the platen. The relative velocity of the pad at one point relative to the wafer is given by Eq. (1) [29]

$$\begin{aligned} v &= \omega_p \times (e + r) - (\omega_w \times r + v_R) \\ &= \omega_p \times e + (\omega_p - \omega_w) \times r - v_R \end{aligned} \quad (1)$$

where ω_p and ω_w represent the angular speed of the platen and the wafer carrier, respectively, v_R represents the translational velocity of the wafer carrier, and e is the center distance between the platen and the wafer carrier.

By calculating velocity integral during the entire polishing time, the sliding distance of each point of the wafer can be given as follows:

$$S(r, \theta) = \int_0^t v(t)_{|(r, \theta)} dt \quad (2)$$

Kinematic analysis reveals that the basic kinematic parameters significantly affect the velocity distribution, the sliding distance distribution, and the nonuniformity [7, 30–33]. Zhao et al. [29] found that the intrinsic relations, especially the coupling relations among the basic motions, i.e., the rotary speed ratio of the wafer to the pad α and the period ratio of the reciprocating motion of the wafer to the rotary motion of the platen

k_{T0} , significantly affect the uniformity of the sliding distance of the wafer relative to the pad, and the distribution of the particle sliding trajectories [34]. For better uniformity, the speed ratio should be close to 1 (but should not equal to 1), and the reciprocating motion of the carrier is necessary.

3.2 Contact stress analysis

The contact stress at the wafer–pad interface largely represents the mechanical action and significantly affects the material removal. Researchers have studied the contact stress distribution of CMP based on a two-dimensional axisymmetric quasi-static finite element model, as shown in Fig. 7(a). The wafer is loaded by the carrier through a flexible carrier film. Early finite element analysis (FEA) calculation of the interfacial von Mises stress of CMP found that the wafer edge has a stress concentration, and the stress distribution corresponds to the profile of the oxide removal rate (see Fig. 8) [8, 35]. The elastic modules of the pad and the carrier film have obvious effects on the stress distribution [36–39]. Besides, the parameters of the wafer, such as wafer dimension, wafer thickness, and surface curvature may affect the contact stress [40]

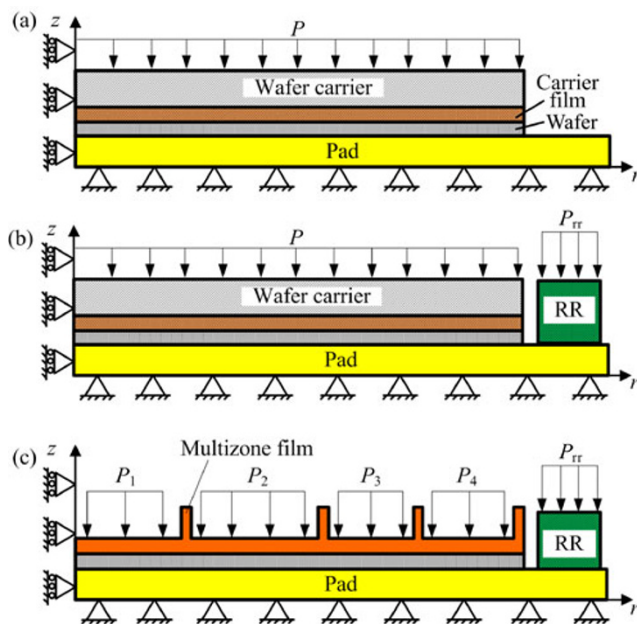


Fig. 7 Two-dimensional axisymmetric finite element model: (a) without retaining ring, (b) with retaining ring, and (c) with multizone carrier film.

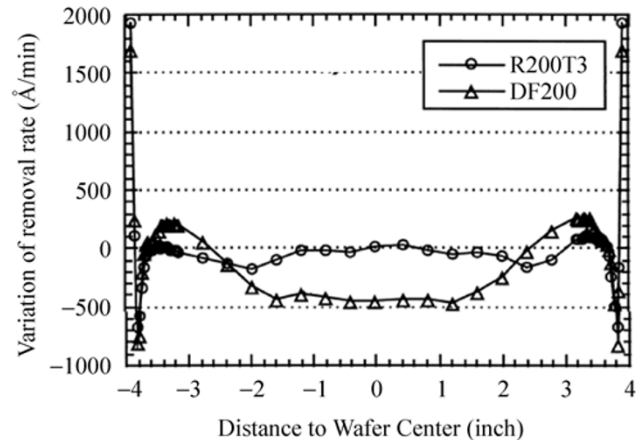


Fig. 8 Profile of material removal rate of oxide (Reproduced from Ref. [35], by permission of The Electrochemical Society).

Compared to the FEA results, Fu et al. [41] gave an approximate analytical solution to the two-body interaction problem. The model reveals that uniform pressure on the wafer backside will still result in a non-uniform contact stress and edge effect.

The retaining ring plays an important role in CMP, and should be considered in the FEA model (see Fig. 7(b)). The ring gap and ring pressure both affect the contact stress (especially the contact stress at the wafer edge). The peak value of the von Mises stress can be decreased by increasing the ratio of the ring load [10]. Using a suitable ring pressure and ring gap, a more uniform contact stress can be obtained relative to the case of no ring pressure [42].

For an actual multizone wafer carrier, the back pressure is divided into several individual zones (see Fig. 7(c)). Wang et al. [11] investigated the contact stress of the multizone carrier, and found that both the contact stress and the MRR of the wafer can be adjusted by varying the applied load at the zones and the retaining ring in multizone CMP. The contact stress at one zone was strongly related to the applied pressure of the loading zone and was slightly affected by the adjacent zones. Figure 9 gives one example of the zone pressure loading effect (Fig. 9(a)) and its effect on the MRR (Fig. 9(b)) when a larger or small pressure is applied to zone 2, respectively. The MRR profile of the wafer exhibited the same trend as the contact stress on the wafer surface [11].

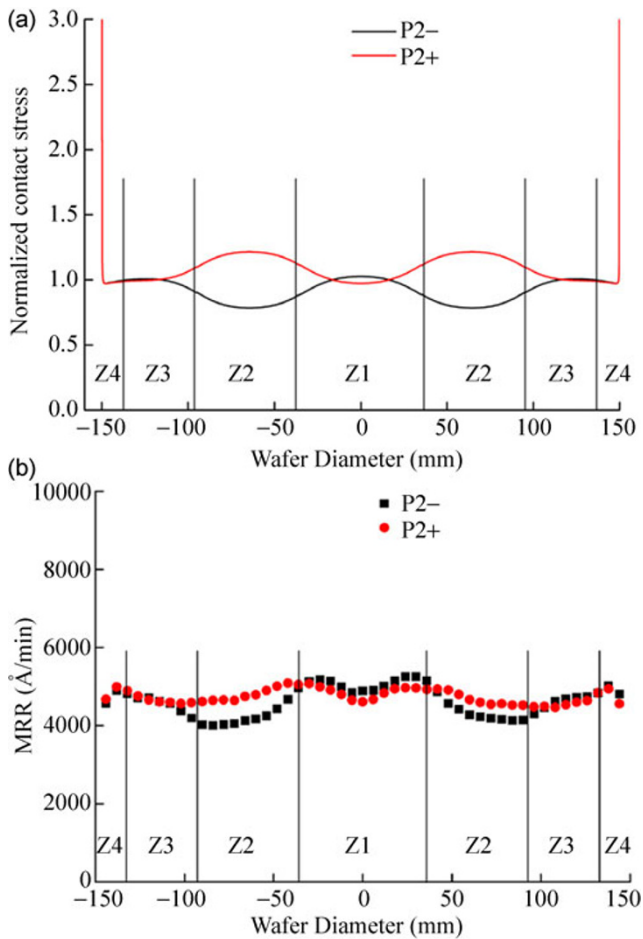


Fig. 9 Zone pressure loading effect and its effect on the MRR when a larger or small pressure is applied to zone 2, respectively: (a) The contact stress, and (b) MRR profiles (Reprinted from Ref. [11], Copyright 2011, with permission from Elsevier).

4 Modeling of CMP

The mechanism and modeling of CMP have been an attractive area of research for many years. Early CMP models were empirically summarized from the industrial production. In addition, some theoretical models that considered the mechanical action from the viewpoint of the contact mechanism, fluid mechanism, or both of them were developed. Further, as the chemical action is an indispensable component in the CMP process, the models that considered the chemical action were also developed.

4.1 Empirical model

The early CMP model which was derived from the

experimental data used an empirical equation to evaluate the effect of the macroscopical polishing variables on the MRR. The most famous model is the Preston equation [28], which describes the linear relationship between the MRR and the product of the downforce P and the relative velocity V , as shown in Eq. (3).

$$\text{MRR} = kPV \quad (3)$$

where k is an empirical constant based on experimental data. P , V , and MRR have an average value. The Preston equation mainly considers the mechanical action and the MRR. Therefore, it has some limitations. In fact, P and V may have a nonlinear relationship with MRR under some conditions. Tseng and Wang [43] re-examined the pressure and speed dependences on the removal rate, and conducted a more precise Preston equation:

$$\text{MRR} = kP^{5/6}V^{1/2} \quad (4)$$

The $V^{1/2}$ term indicates a much weaker dependence of the removal rate on the speed V . A higher speed may be considered to imply a larger centrifugal force for the slurry and a larger hydrodynamic pressure at the wafer-pad interface [44]. Therefore, the MRR may not always increase linearly with the speed.

Then, modified Preston equations in the form of $\text{MRR} = kP^\alpha V^\beta$ were proposed. Unfortunately, each equation has limitations because they are empirical equations that are based on limited experimental data. A more accurate local relevant expression for the MRR is more reasonable [45]:

$$\text{MRR}(x, y) = kP(x, y)V(x, y) \quad (5)$$

Using Eq. (5), the MRR of one point on the wafer surface can be achieved by calculating the integral of P and V during the whole polishing time.

4.2 Modeling from perspective of mechanism

4.2.1 Model based on contact mechanism

The most important elements that contribute to material removal during CMP include the abrasive particles, slurry chemicals, and polishing pad. The abrasive-wafer interaction, chemical-wafer interaction, and

wafer–pad interaction all play the important roles in CMP. The contact mechanism model ignores the fluid action. The downforce applied on the polishing pad is assumed to be carried by the solid–solid contact of the wafer surface, i.e., the abrasive–wafer interaction and asperity–wafer interaction. The interactions consist of three different models based on the dimensions [46, 47], namely the particle scale model, asperity scale model, and wafer scale model, as shown in Fig. 10. The particle scale model and asperity scale model are the bases used to access the wafer scale model.

(a) Particle scale model

The particle scale model evaluates the indentation depth and the wear volume of the particle. A single particle wear model was proposed by Zhao et al. [48, 49], as shown in Fig. 11. Because the pad is much softer than the hard particles, the particle will be indented into the pad. The indentation depth and section area of a single particle can be calculated based on the theory of contact mechanics in conjunction with the force equilibrium.

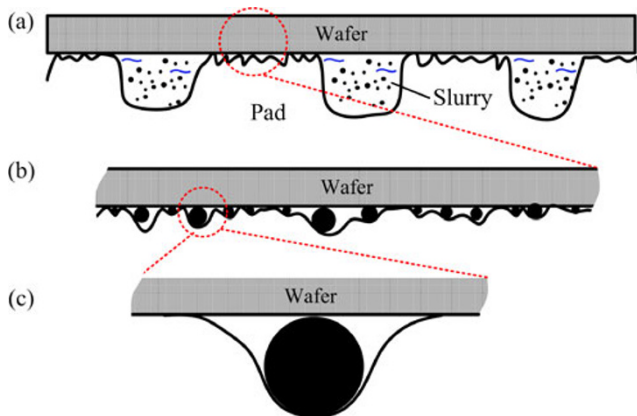


Fig. 10 CMP model at different scales: (a) wafer scale, (b) asperity scale, and (c) particle scale (Reproduced from Ref. [6], by permission of The Electrochemical Society).

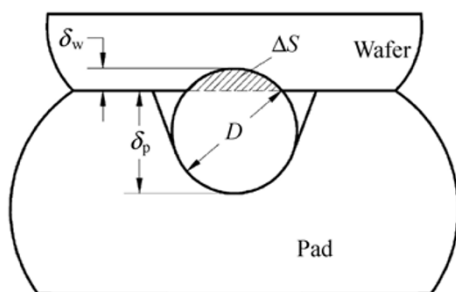


Fig. 11 Single particle contact model (Reprinted from Ref. [48], Copyright 2002, with permission from Elsevier).

Zhao's model gives the wear volume of the wafer by a single particle as

$$\Delta G = K\Delta S V t \quad (6)$$

where K is the wear constant, ΔS is the cross section area of the worn groove, V is the relative velocity between the wafer and the pad, and t is the polishing time. The pad properties affect the contact status of the particles, and should be considered in the model [50]. Shi et al. [51] and Wang et al. [52] compared the different contact statuses for the soft pad and hard pad (see Fig. 12). For the hard pad (Fig. 12(a)), the particles make contact with the wafer surface, while the pad asperities do not; for the soft pad (Fig. 12(b)), the particles are embedded in the pad asperities, and both the particles and the pad asperities make contact with the wafer surface. Therefore, the removal rate model is quite different for the soft pad and hard pad. The relationship between the removal rate and the particle size was further developed [53].

(b) Asperity scale model

In the asperity scale model, one or more particles are trapped at the wafer–asperity interface. Only the particles embedded in the asperity contribute to material removal in CMP, and they can therefore be defined as active particles [54]. The asperity deformation and contact area are calculated to evaluate the

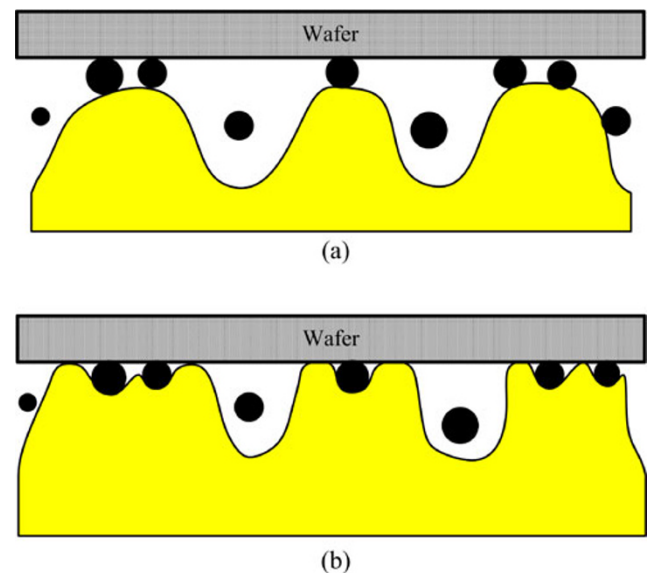


Fig. 12 Contact status of (a) hard pad, and (b) soft pad (Reprinted from Ref. [51], with kind permission from Springer Science + Business Media).

number of active particles, and to further evaluate the MRR. Zhao et al. [49] studied the contact model of a single asperity for elastic, plastic, and elastic-plastic statuses. Their results reveal that the pad property and topography have an important effect on the efficiency on the material removal.

(c) Wafer scale model

The atomic scale model and asperity scale model are both local models. In order to obtain the MRR model across the entire wafer surface, it is necessary to expand the local models to the wafer scale. The wafer scale model uses a mathematical statistical method to calculate the actual contact area across the wafer and to evaluate the number of active particles. Using the particle scale model as the element, the global MRR model can be obtained.

The pad asperity is randomly distributed, as shown in the left figure of Fig. 13. The right figure of Fig. 13 gives a description of the probability density distribution of the pad height. A classic probability statistical model for the rough surface, G-W model [55], is selected to evaluate the actual contact area between the wafer and the pad.

$$A = \pi N \beta \int_d^{\infty} (z-d) \phi(z) dz \quad (7)$$

where N is the total number of asperity, $\phi(z)$ is the probability density distribution function of the pad asperity height, β is the characteristic length scale for the roughness of the pad surface, z is the pad height, and d is the distance to the mean line of pad surface.

The number of active particles is evaluated base on several hypotheses [50]. Zhao's model [48] assumes that the particles in the contact area have the same face density with the slurry, while Jeng's model [56] assumes that particles with the same number of that in the slurry with the volume of the compress asperities were trapped at the wafer-pad interface. The precision

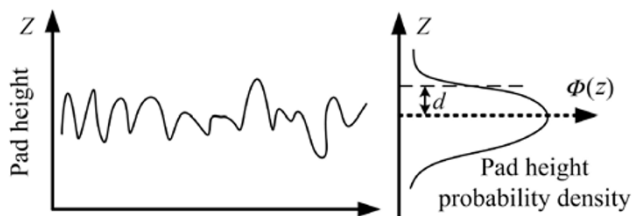


Fig. 13 Probability density distribution of the pad height.

of the model is determined by the above assumptions. In fact, the actual contact ratio is very small (<1%) [54, 57].

4.2.2 Model considering fluid mechanism

Fluid lubrication plays an important role in the wafer-pad interactions. The fluid force can support a part of the downforce. Assume that s is the complex roughness and h is the fluid film thickness. Based on lubrication theory, if $h \gg s$, full film lubrication is generated and Reynolds equation can be used to solve the fluid pressure, while if $h \approx s$, mixed lubrication is generated and the roughness of the surface cannot be ignored. Some researchers have used simplified lubrication models and the Reynolds equation to solve the fluid pressure for CMP.

The full film CMP lubrication model was first introduced to CMP and assumes that the wafer has been absolutely separated by a slurry film. The most simplified CMP lubrication model ignored the deformation of the wafer and the pad (as shown in Fig. 14(a)). Based on the cylindrical coordinate Reynolds equation and the equations for the force and torque, the fluid pressure of the slurry film was calculated using numerical methods. The results suggested a positive pressure, with the center pressure being much larger than the pressure at the edge [58–60]. Sundararajan et al. [61] further considered the deformation of the wafer in the model, as shown in Fig. 14(b). Thakurta et al. [14] further considered the deformation of the pad, as shown in Fig. 14(c). Also, a positive pressure was obtained.

Actually, the pad surface is not flat, but has a specific roughness and micropores. The pad surface profile will affect the lubrication, especially when the roughness is comparable to the film thickness. Kim et al. [62] and Ng et al. [63] added the pad roughness to the model and introduced the flow factor to the average Reynolds equation. This kind of model is close to the actual condition, however, the pad profile is difficult to model.

For general CMP, the asperity/particle must be in contact with the wafer. Therefore, the mixed lubrication model is more suitable for CMP [64]. Tichy et al. [65] simulated the regular distribution of the pad asperities, as shown in Fig. 15(a). Tsai et al. [66] assumed that a

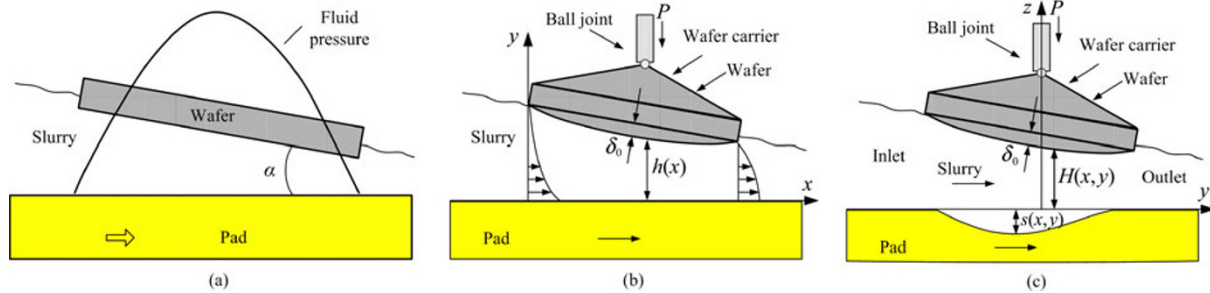


Fig. 14 Lubrication models of CMP: (a) rigid pad/wafer, (b) considering wafer deformation (Reproduced from Ref. [61], by permission of The Electrochemical Society), and (c) considering wafer and pad deformation (Reprinted from Ref. [14], Copyright 2000, with permission from Elsevier).

part of the wafer is in contact with the pad, while a part of the wafer has a hydrodynamic lubrication with the pad, as shown in Fig. 15(b). Using the mixed lubrication model of CMP, the fluid pressure, the fluid film thickness, and the contact ratio can be obtained.

The relative motion is another important factor that affects the lubrication during CMP. The friction torque at the interface produced by the relative motion will cause the wafer to lean and change the wafer orientation. As a result, the contact force will be nonuniform. If there is no retaining ring around

the wafer, the friction torque will drag the leading edge down toward the pad, and the wafer's leading edge has a much tenser contact with the pad. Therefore, a suction pressure is formed in the leading region of the wafer owing to a diverging clearance [65]. In the above models, the simplification of the carrier structure, especially the retaining ring, may obviously affect the contact feature of the wafer [9, 10, 67], which may further affect the slurry flow and the lubrication behavior between the wafer and pad. It is desired that more practical model considering the carrier structure and loading characteristic will be developed.

4.3 Molecular dynamics simulation of CMP: atomic view

To study the physical process of material removal by abrasive particles during CMP on an atomic scale, molecular dynamic (MD) simulations were widely used to analyze the material removal process caused by the silica cluster on the silicon substrate under different conditions. The extruding effect, the sliding effect, and the rolling effect were all found to affect material removal and surface polishing [68–74].

A basic silica cluster impact simulation was carried out in dry conditions by Chen et al. [71]. When a silica cluster impacts on the crystal silicon substrate with a suitable velocity and incidence angle, the silicon surface is extruded (as shown in Fig. 16) due to the combined effects of thermal spread, phase transformation, and crystallographic slip, with the thermal spread being the most significant. A higher impacting speed results in a larger extrusion of the substrate.

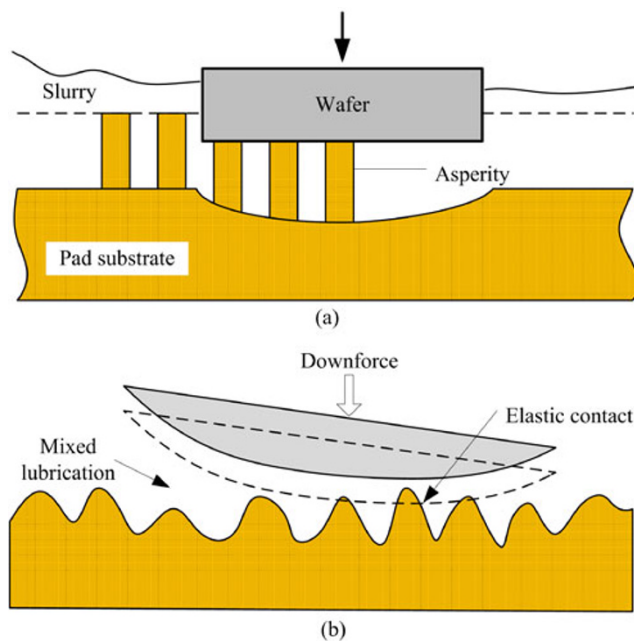


Fig. 15 Mixed lubrication model of CMP: (a) Tichy's model (Reproduced from Ref. [65], by permission of The Electrochemical Society), and (b) Tsai's model [66].

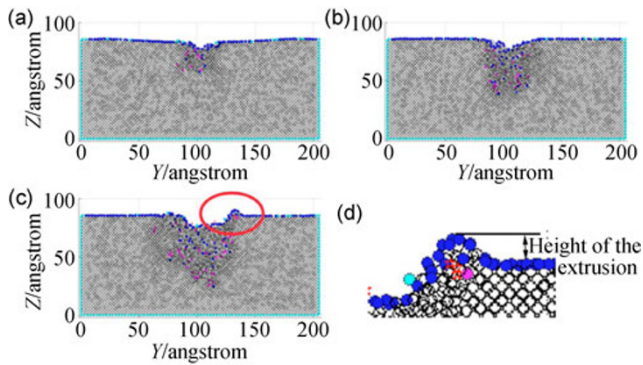


Fig. 16 Section view of atoms after normal impacting by 5184 cluster at different impact velocities: (a) 2,500 m/s, (b) 4,313 m/s, (c) 6,000 m/s, and (d) enlarged drawing of an extrusion after the impact in Fig. (c) (Reprinted from Ref. [71], Copyright 2011, with permission from Elsevier).

During CMP, the wafer surface is exposed in the slurry. Therefore, the particle–wafer interaction takes place in wet conditions. The surface damage in the wet condition was further simulated using the MD method for comparison with the dry condition [69, 70]. The damage to the substrate after the dry impact is more severe than that after the wet impact under the same other conditions, and it is especially obvious for large incidence angles. The water film will affect the energy transfer process for the wet impact as compared to the dry impact.

During CMP, the particle clamped between the wafer and the pad may slide and roll when the pad moves relative to the wafer. Using the MD method, the sliding effect was investigated by Han et al. [75], and the abrasive rolling effect on the material removal and the surface finish in the CMP process was studied by Si et al. [73]. In Si's model, an external downforce was applied to the particle on the substrate, and drove the particle to roll forward under a lateral driving force. Their results show that the silica particle will roll across the silicon substrate. Meanwhile, some atoms of the substrate are dragged out and adhered to the silica particle, leaving some atomic vacancies on the substrate surface, as shown in Fig. 17. As a result, a high quality surface can be obtained.

Si et al. [73] further described the material removal mechanism. During the rolling process, the material was mainly removed by adhering wear. As shown in Fig. 18(a), under the external down force and the driving force, some atoms of the silicon substrate

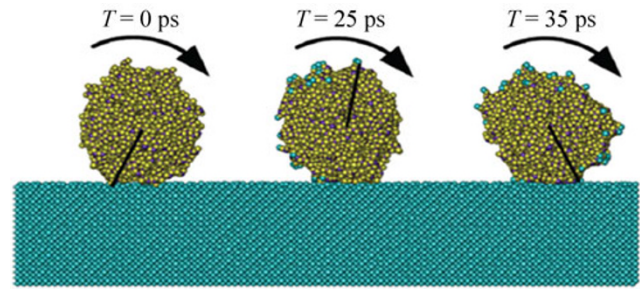


Fig. 17 MD simulation results of the silica particle rolling process under an external downforce of 5 nN and a lateral driving force of 10 nN (Reprinted with permission from Ref. [73]. Copyright 2011, American Institute of Physics).

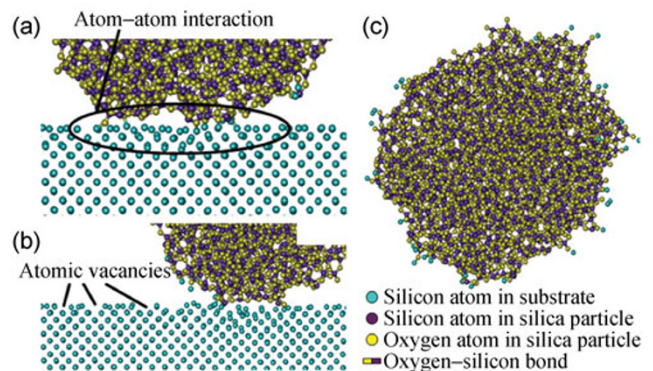


Fig. 18 Material removal characteristics in abrasive rolling process: (a) atom–atom interactions between the atoms of the silicon substrate and the silica particle, (b) atomic vacancies on the silicon substrate after rolling, and (c) silica particle after rolling across the silicon substrate (Reprinted with permission from Ref. [73]. Copyright 2011, American Institute of Physics).

and the silica particle formed stronger atom–atom interactions. As the silica particle rolled forward, some of the Si–Si bonds on the substrate surface were broken and the Si atoms were dragged out from their original positions and adhered to the silica particle, as shown in Fig. 7(c).

From the above discussion, we propose that abrasive extruding, sliding, and rolling play important roles in material removal in the abrasive CMP of the silicon substrate. If the chemicals were considered in the MD model, the simulation results could be closer to those of the actual CMP process.

4.4 Modeling of chemical-mechanism synergy during CMP

The mechanical models are not sufficiently accurate

as they ignored the chemical action, which is an important part of CMP. Luo and Dornfeld [50] give a general model which considers the chemical corrosion:

$$\text{MRR} = \rho_w NV_{\text{removed}} + C_0 \quad (8)$$

where ρ_w is the density of the wafer, N is the number of the active particles, V_{removed} is the removal rate of a single particle, and C_0 represents the removal rate caused by chemical corrosion. This model considers both the mechanical action and chemical action in CMP. However, it is not accurate to use a constant to describe the corrosion.

In another general accepted model, a thin film is generated on the wafer surface, which is soft and can be easily removed. The film is removed by the mechanical action of the particle. The film generation and removal are parts of a dynamic process. When the growth rate and the removal rate attain some equilibrium, the best polishing results are obtained [76, 77].

In fact, the chemical action and mechanical action have a synergistic effect, in which they are both promoted. Li et al. [78, 79] considered the interaction of mechanical part and chemical part in their model. Based on the corrosion and wear theory, a mathematical material removal model incorporating both chemical and mechanical effects during CMP was proposed.

During CMP, the slurry has an (electro-) chemical erosion effect on the wafer surface, and the particles also have a mechanical abrasive wear effect on the wafer surface. The synergistic effect of the (electro-) chemical corrosion effect and the mechanical abrasive wear effect result in a high efficiency MRR and good surface quality to CMP. The CMP system is similar to a corrosion-wear system. Li et al. [79] gives a synergy model which expresses the total MRR using the mechanical component r_{wc} and chemical component r_{cc} :

$$\text{MRR} = r_{wc} + r_{cc} \quad (9)$$

where

$$r_{wc} = r_w + r_{c-w} \quad (10)$$

and

$$r_{cc} = r_c + r_{w-c} \quad (11)$$

where, r_w and r_c represent the removal rate due to

pure wear and pure corrosion, respectively; r_{c-w} and r_{w-c} represent the part of corrosion-induced wear, and the part of wear-induced corrosion, respectively. Therefore, in Li's model, r_{c-w} and r_{w-c} gives the synergism of the wear and corrosion, which results in the greatest material removal during CMP.

Based on the mechanical model, the real wafer-pad contact area can thus be evaluated. By multiplying the number of active particles with the removal volume of a single particle, Li gives an expression for the MRR due to abrasive wear. When the film on the wafer surface is removed by particles, a fresh wafer surface is exposed, which promotes the dissolution of the copper. As a result, the anodic current subsequently increases due to the enhanced dissolution of the wafer surface. Hence, the MRR due to corrosion during CMP can be calculated by Faraday's law. Finally, Li gives the total MRR as follows:

$$\text{MRR} = r_{wc} + r_{cc} = \frac{C_1}{C_0^2 R^2} (h^2 + C_2 C_3 h) P_0^{2/3} v + C_3 i_0 \quad (12)$$

Li's model not only quantifies the chemical mechanical synergy, but also isolates each component's contribution to the MRR. Li's model reveals that major factors affecting the material removal include the process parameters, properties of the pad, particle, and slurry (pH, concentration).

In order to assess the relative importance of mechanical wear and chemical corrosion to the MRR during CMP, Li gives a parameter of the mechanical-to-chemical ratio (r_{wc}/r_{cc}).

$$\frac{r_{wc}}{r_{cc}} \propto RP^{1/3} \quad (13)$$

where R is the particle size. Equation (13) indicates that the mechanical-to-chemical ratio increases linearly with particle size, and that an increase in the applied pressure will enhance the mechanical effect.

Figures 19(a) and 19(b) show the corrosion-wear maps [79] from Li's model according to the applied pressure and the particle size, respectively. These maps reveal that the chemical-mechanical synergy dominates the material removal during CMP. As the applied pressure and particle size increase, there is the appearance of a transition mechanism from corrosion-induced wear to wear-induced corrosion [79].

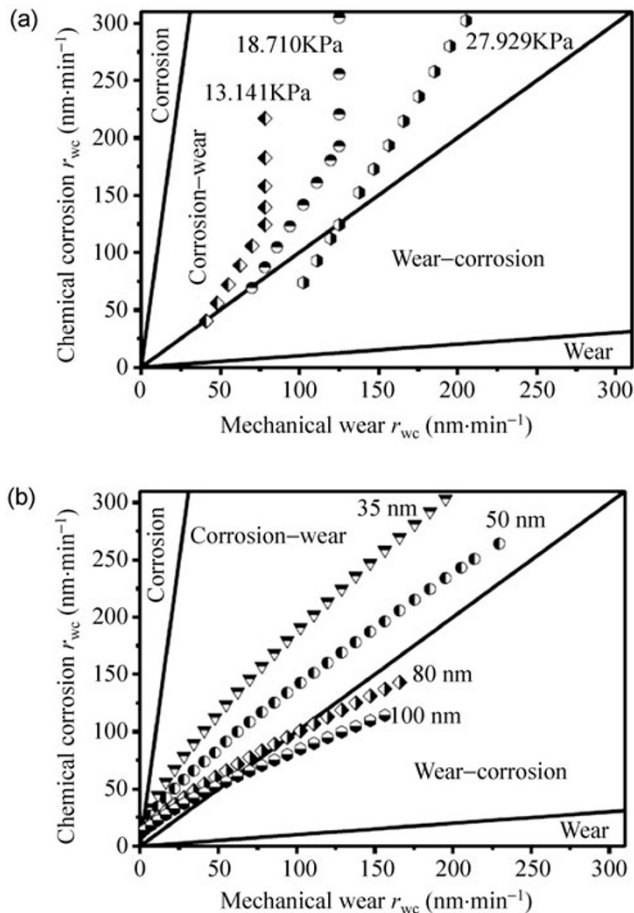


Fig. 19 Corrosion–wear mechanism regime map with chemical corrosion vs. mechanical wear: (a) mechanism of different applied pressures, and (b) mechanism of different particle sizes (Reproduced from Ref. [79], by permission of The Electrochemical Society).

5 Experimental study of CMP

5.1 Nano-scale material removal experiments

Atomic Force Microscope (AFM) has been widely used to study the effects of the particle wear effect and the effect of slurries on the mechanical removal of the surface layer. Yu et al. [80] found that the tribochemical wear of the silicon surface occurred for the SiO₂ tips and single-crystalline silicon wear pair, even at contact pressures that are much lower than the hardness. The surface topography of an etched Cu sample with or without probe scratching can be investigated by AFM. Liao's [81] comparative AFM scratch tests for copper samples after exposure to different solutions (see Fig. 20) revealed that the MRR and surface roughness are significantly influenced by the chemicals and pH

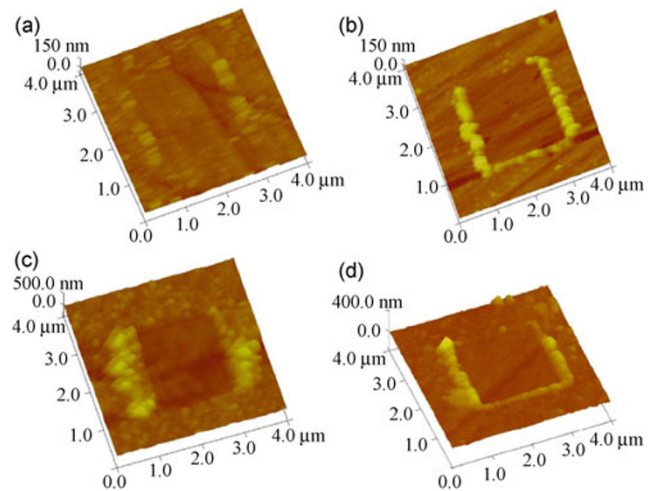


Fig. 20 AFM of the scratched area morphology of copper samples after exposure to different solutions at pH 4 for 8 min: (a) virgin Cu, (b) solution No. 1 containing 5 wt% H₂O₂, (c) solution No. 2 containing 5 wt% H₂O₂ and 1 wt% glycine, and (d) solution No. 3 containing 5 wt% H₂O₂, 1 wt% glycine, and 0.1 wt% BTA (Reprinted from Ref. [81], with kind permission from Springer Science + Business Media).

value of the slurry. The scratched depth of all of the etched Cu samples was greater than that of the virgin Cu sample. For solution No. 1 containing 5 wt% H₂O₂, the scratched depth was about two times greater than that of the virgin Cu. For solution No. 2, the combination of H₂O₂ and glycine greatly increased the scratched depth. However, for solution No. 3 with a further addition of BTA, the scratched depth was lower than that of solution No. 2, which suggested that BTA not only inhibited the chemical dissolution of copper, but also inhibited the mechanical removal of copper.

5.2 Material removal regime of CMP

Luo and Dornfeld [82] have given a map of material removal regions according to the abrasive weight concentration. It is also important to give the material removal regime from the aspect of the slurry chemical property.

To determine the material removal regime of copper CMP from the perspective of the roles of chemical corrosion, abrasive wear, and their synergistic effects on the material removal, Li et al. [78] used electrochemical analysis and a nano-scratching method to investigate the MRR and surface quality after CMP with slurries having different pH values. They calculated the mechanical–chemical removal rate ratio based on the

experimental data, and finally constructed a removal mechanism map for copper CMP depending on the pH values, as shown in Fig. 21. The pure chemical effect accounts for almost all of the material removal at pH 3.0 and 10.0, indicating that the chemical corrosion effect plays a dominant role during the CMP process; in the alkaline slurry, the wear–corrosion effect predominates in the material removal at pH values of 8.0 and 9.0, while the copper removal mechanism transfers to corrosion–wear action in the acidic slurry from pH 4.0 to 6.0. The wear-induced corrosion effect resulted in a majority of the material removal from a pH of 7.0 to 9.0, and a good surface quality was obtained. Li's results provide strategies for realizing the process optimization of CMP.

5.3 *In situ* study of fluid lubrication behavior during CMP

The slurry plays an important role at the wafer–pad interface during CMP. The particles and chemicals are brought to the interface with the slurry flow [83]; the slurry can build a lubrication film and decrease the friction force, and the fluid pressure can bear some of the downforce, thus causing wafer to have a flexible landing on the pad.

To experimentally determine the fluid behavior at the wafer–pad interface, several fluid pressure mapping studies were performed on the simplified experimental setups of CMP, using a disk to simulate the wafer and

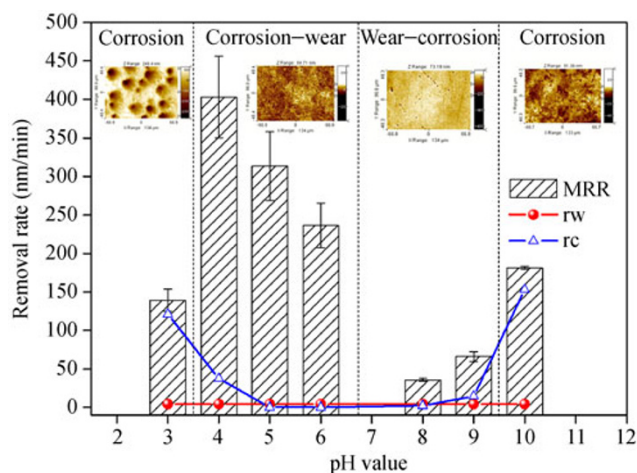


Fig. 21 Li's material removal mechanism map for copper CMP (Reprinted from Ref. [78], with kind permission from Springer Science+Business Media).

wafer carrier [84–89]. Their experiments found that a large negative pressure region occupying more than 70% of the contact area between the disk and the pad existed near the leading edge of the disk. However, as the rigid disk is quite different from the wafer with respect to its bending property, the results may be quite different from those for real situations.

To study the fluid lubrication behavior during an actual CMP process which uses the multizone carrier and the retaining ring, Zhao et al. [90–92] developed a novel *in-situ* fluid pressure and wafer status measurement system, which uses an array of pressure sensors to measure the fluid pressure, and an array of distance sensors to monitor the wafer status. The *in situ* measurement system was integrated in a 12-inch CMP equipment. The schematic section view of the integrated measurement system is shown in Fig. 22.

Zhao's fluid pressure measurements revealed the presence of a small negative pressure region at the leading edge, while the positive pressure is dominant (see Fig. 23), which is quite different from the test results obtained from the simplified CMP test tool. The fluid pressure can support 10%–30% of the downforce depending on the downforce [44]. Wafer bending/orientation measurements reveal a micron level wafer bending and a slight wafer pitch angle during the dynamic polishing process, both of which increase linearly with the downforce.

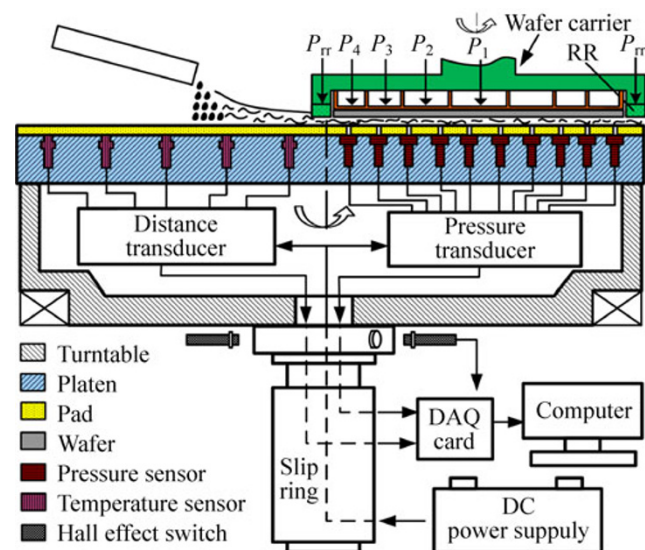


Fig. 22 Schematic of *in situ* measurement system of CMP (Reprinted from Ref. [92], Copyright 2013, with permission from Elsevier).

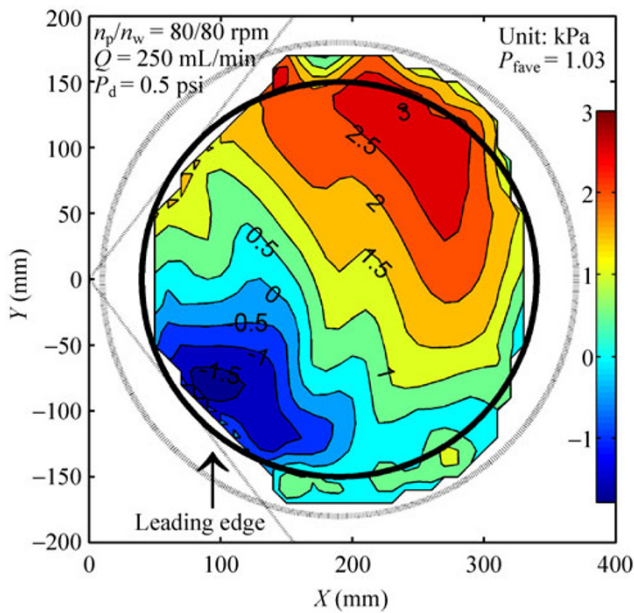


Fig. 23 Fluid pressure distribution across the 12-inch wafer at 0.5 psi downforce, 80/80 rpm carrier/platen speed, and 250 mL/min slurry flow rate (Reproduced from Ref. [90], by permission of The Electrochemical Society).

Zhao et al. [91] gave a reasonable explanation from the viewpoint of the wafer-pad contact status and contact stress, as shown in Fig. 24. The convexly bent and trailing edge pitched wafer produce a convergent-dominated wedged gap between the wafer and the pad, and generate a positive dominated fluid pressure. The edge stress concentration effect causes a small negative pressure at the leading edge.

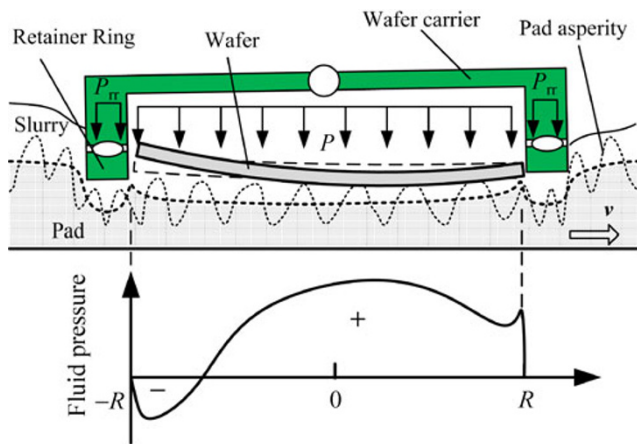


Fig. 24 Schematic of wafer-pad interaction and fluid lubrication (Reprinted from Ref. [91], Copyright 2013, with permission from Elsevier).

5.4 Process capability

Figure 25 gives one optimized process results of the MRR profile using a five-zone wafer carrier. The platen/carrier speed is 90/87 rpm and the slurry flow rate is 300 mL/min. The pressure applied to zones 1–5 and retaining ring (see Fig. 5(c)) are 1.0, 1.0, 1.1, 2.1, 3.3, and 3.6 psi, respectively. The average MRR is close to 5,000 Å/min (in fact, the MRR can increase to 6,000–7,000 Å/min when the downforce increases to 2 psi), the standard deviation (STD) of the MRR is 74 Å/min, and the nonuniformity is 1.49%. After CMP, the surface roughness is easily to be decreased to sub-nanometer. The recent reported results show that, using an optimized silicon slurry and an optimized polishing process, the minimum surface roughness after CMP can achieve 0.05 nm (Ra, measured by AFM) [93]. The process potentiality is still developing toward to the unknown ultimate.

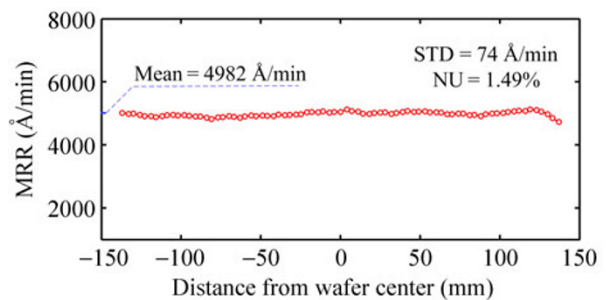


Fig. 25 MRR profile at downforce of about 1psi, platen/carrier speed of 90/87 rpm, and slurry flow rate of 300 mL/min.

6 Conclusions

For several decades, chemical mechanical polishing (CMP) has been developed from both a theoretical and technical perspective. The mechanism of CMP is shown based on theoretical modeling and experimental verification, but it still requires further development. The following conclusions have been made from this review.

(1) The reduction in the feature size of IC products, the increase in wafer dimensions, and the use of low- k materials all result in further challenges to CMP. More precision technologies, such as the pressure control technology and the end point detecting technology,

are significant for CMP process control.

(2) CMP is a complex mechanism. Many factors related to the carrier structure, the polishing pad, the slurry, and the process parameters may affect the final polishing results. The wafer–pad interfacial status, including the pressure/stress distribution, the slurry film distribution, the sliding distance distribution, and the temperature distribution play important roles in determining the final polishing results.

(3) The kinematics and the contact stress are the most basic aspects that describe the mechanical interactions between the wafer and the pad. The mechanical models ranging from the particle scale to the wafer scale based on the contact mechanism analysis and the kinematic analysis can be used to predict the profile from a mechanical viewpoint. Moreover, the MD simulations from the atomic scale reveal the physical mechanism of the particle–substrate action, which suggests that the extruding, sliding, and rolling of the particles affect the material removal.

(4) The CMP mechanism is complex because both the chemical and mechanical actions contribute to CMP and these actions are affected by many factors. From the viewpoint of the mechanism, including the contact mechanism and the fluid mechanism, the models cannot fully reveal the CMP mechanism, but are useful in the profile prediction to some degree. Considering the chemical and mechanical synergistic effects, the models are closer to the actual mechanism of CMP. The model of the chemical mechanical synergy reveals that both the chemical and mechanical actions can assist each other in material removal.

(5) Experimental approaches to the CMP mechanism of material removal and planarization further confirm that the chemicals in the slurry affect the film property and the particle wear volume. The pH value significantly affects the material removal regimes of CMP. Corrosion–wear action in the acidic slurry with pH ranging from 4.0 to 6.0 will transfer to a wear-induced corrosion effect when the pH increases to 7.0–9.0.

Acknowledgements

The authors appreciate the financial support provided by the Science Fund for Creative Research Groups

(Grant No. 51021064), and the National Natural Science Foundation of China (Grant No. 51305227). The authors would like to thank Enago (www.enago.cn) for the English language review.

Open Access: This article is distributed under the terms of the Creative Commons Attribution License which permits any use, distribution, and reproduction in any medium, provided the original author(s) and source are credited.

References

- [1] Kahng A B, Samadi K. CMP fill synthesis: a survey of recent studies. *IEEE T Comput Aid D* **27**(1): 3–19 (2008)
- [2] Ryan J G, Geffken R M, Poulin N R, Paraszczak J R. The evolution of interconnection technology at IBM. *Ibm J Res Dev* **39**(4): 371–381 (1995)
- [3] Bai P, Auth C, Balakrishnan S, Bost M, Brain R, Chikarmane V, Heussner R, Hussein M, Hwang J, Ingerly D, James R, Jeong J, Kenyon C, Lee E, Lee S H, Lindert N, Liu M, Ma Z, Marieb T, Murthy A, Nagisetty R, Natarajan S, Neirynck J, Ott A, Parker C, Sebastian J, Shaheed R, Sivakumar S, Steigerwald J, Tyagi S, Weber C, Woolery B, Yeoh A, Zhang K, Bohr M. A 65nm logic technology featuring 35nm gate lengths, enhanced channel strain, 8 Cu interconnect layers, low-*k* ILD and 0.57 μm^2 sram cell. In *Electron Devices Meeting, 2004. IEDM Technical Digest. IEEE International*, 2004: 657–660.
- [4] Zantye P B, Kumar A, Sikder A K. Chemical mechanical planarization for microelectronics applications. *Mat Sci Eng R* **45**(3–6): 89–220 (2004)
- [5] Bohr M. Silicon technology for 32nm and beyond system-on-chip products. In *Intel Developer Forum*, 2009.
- [6] Bozkaya D, Muftu S. A material removal model for CMP based on the contact mechanics of pad, abrasives, and wafer. *J Electrochem Soc* **156**(12): H890–902 (2009)
- [7] Kim H J, Jeong H D. Effect of process conditions on uniformity of velocity and wear distance of pad and wafer during chemical mechanical planarization. *J Electron Mater* **33**(1): 53–60 (2004)
- [8] Srinivasa-Murthy C, Wang D, Beaudoin S P, Bibby T, Holland K, Cale T S. Stress distribution in chemical mechanical polishing. *Thin Solid Films* **308–309**: 533–537 (1997)
- [9] Lo S P, Lin Y Y, Huang J C. Analysis of retaining ring using finite element simulation in chemical mechanical polishing process. *Int J Adv Manuf Tech* **34**(5–6): 547–555 (2007)

- [10] Lin Y Y. Influence of a retaining ring on strain and stress in the chemical mechanical polishing process. *Mater Manuf Process* **22**(7–8): 871–878 (2007)
- [11] Wang T Q, Lu X C. Numerical and experimental investigation on multi-zone chemical mechanical planarization. *Microelectron Eng* **88**(11): 3327–3332 (2011)
- [12] Park K, Oh J, Jeong H. Pad characterization and experimental analysis of pad wear effect on material removal uniformity in chemical mechanical polishing. *Jpn J Appl Phys* **47**(10Part 1): 7812–7817 (2008)
- [13] Kim B S, Tucker M H, Kelchner J D, Beaudoin S P. Study on the mechanical properties of CMP pads. *IEEE T Semiconduct M* **21**(3): 454–463 (2008)
- [14] Thakurta D G, Borst C L, Schwendeman D W, Gutmann R J, Gill W N. Pad porosity, compressibility and slurry delivery effects in chemical-mechanical planarization: modeling and experiments. *Thin Solid Films* **366**(1–2): 181–190 (2000)
- [15] Rosales-Yeomans D, DeNardis D, Borucki L, Philipossian A. Design and evaluation of pad grooves for copper CMP. *J Electrochem Soc* **155**(10): H797–H806 (2008)
- [16] Lee H, Park B, Jeong H. Influence of slurry components on uniformity in copper chemical mechanical planarization. *Microelectron Eng* **85**(4): 689–696 (2008)
- [17] Steigerwald J M, Murarka S P, Gutmann R J, Duquette D J. Chemical processes in the chemical mechanical polishing of copper. *Mater Chem Phys* **41**(3): 217–228 (1995)
- [18] Information. <http://www.itrs.net/Links/2012ITRS/Home2012.htm>, 2012.
- [19] Peter S. Low-pressure CMP developed for 300 mm ultralow-*k*. *Semiconductor International* **26**(12): 30 (2003)
- [20] Dhandapani S, Qian J, Cherian B, Menk G, Garretson C, Lee H, Bennett D, Osterheld T. *In situ* profile control with titan edgetm heads for dielectric planarization of advanced CMOS devices. In *International Conference on Planarization/CMP Technology (ICPT 2012)*, Grenoble, France, 2012: 1–5.
- [21] Hocheng H, Huang Y L. A comprehensive review of end point detection in chemical mechanical polishing for deep-submicron integrated circuits manufacturing. *Int J Nano Tech* **1**: 1–18 (2002)
- [22] Das T K, Ganesan R, Sikder A K, Kumar A. Online end point detection in CMP using SPRT of wavelet decomposed sensor data. *IEEE T Semiconduct M* **18**(3): 440–447 (2005)
- [23] Bibby T, Adams J A, Holland K. Optical endpoint detection for chemical mechanical planarization. *J Vac Sci Technol B* **17**(5): 2378–2384 (1999)
- [24] Seo Y J, Lee W S, Park J S, Kim S Y. Motor-current-based real-time end point detection of shallow-trench-isolation chemical mechanical polishing process using high-selectivity slurry. *Jpn J Appl Phys* **42**(10): 6396–6369 (2003)
- [25] Xie Y S, Bhushan B. Effects of particle size, polishing pad and contact pressure in free abrasive polishing. *Wear* **200**(1–2): 281–295 (1996)
- [26] Bastawros A, Chandra A, Guo Y J, Yan B. Pad effects on material-removal rate in chemical-mechanical planarization. *J Electron Mater* **31**(10): 1022–1031 (2002)
- [27] Kim H J, Kim H Y, Jeong H D, Lee E S, Shin Y J. Friction and thermal phenomena in chemical mechanical polishing. *J Mater Process Tech* **130**(SI): 334–338 (2002)
- [28] Oh S, Seok J. Modeling of chemical-mechanical polishing considering thermal coupling effects. *Microelectron Eng* **85**(11): 2191–2201 (2008)
- [29] Zhao D W, He Y Y, Wang T Q, Lu X C. Effect of kinematic parameters and their coupling relationships on global uniformity of chemical-mechanical polishing. *IEEE T Semiconduct M* **25**(3): 502–510 (2012)
- [30] Tseng W T, Chin J H, Kang L C. A comparative study on the roles of velocity in the material removal rate during chemical mechanical polishing. *J Electrochem Soc* **146**(5): 1952–1959 (1999)
- [31] Wang C L, Jin Z J, Kang R K. Effects of kinematic forms on material removal rate and non-uniformity in chemical mechanical planarisation. *Int J Mater Prod Tec* **31**(1): 54–62 (2008)
- [32] Hocheng H, Tsai H Y, Tsai M S. Effects of kinematic variables on nonuniformity in chemical mechanical planarization. *Int J Mach Tool Manu* **40**(11): 1651–1669 (2000)
- [33] Tyan F. Nonuniformity of wafer and pad in CMP: kinematic aspects of view. *IEEE T Semiconduct M* **20**(4): 451–463 (2007)
- [34] Zhao D, Wang T, He Y, Lu X. Kinematic optimization for chemical mechanical polishing based on statistical analysis of particle trajectories. *Semiconductor Manufacturing, IEEE Transactions on* **26**(4): 556–563 (2013)
- [35] Wang D, Lee J, Holland K, Bibby T, Beaudoin S, Cale T. Von mises stress in chemical-mechanical polishing processes. *J Electrochem Soc* **144**(3): 1121–1127 (1997)
- [36] Lin Y Y, Chen D Y, Ma C. Simulations of a stress and contact model in a chemical mechanical polishing process. *Thin Solid Films* **517**(21): 6027–6033 (2009)
- [37] Lin Y Y, Lo S P. Modeling of chemical mechanical polishing process using FEM and abductive network. *Eng Appl Artif Intel* **18**(3): 373–381 (2005)
- [38] Lin Y Y, Lo S P. A study of a finite element model for the chemical mechanical polishing process. *Int J Adv Manuf Tech* **23**(9–10): 644–650 (2004)
- [39] Lin Y Y, Lo S P. A study on the stress and nonuniformity of the wafer surface for the chemical-mechanical polishing process. *Int J Adv Manuf Tech* **22**(5–6): 401–409 (2003)

- [40] Chen K S, Yeh H M, Yan J L, Chen Y T. Finite-element analysis on wafer-level CMP contact stress: reinvestigated issues and the effects of selected process parameters. *Int J Adv Manuf Tech* **42**(11–12): 1118–1130 (2009)
- [41] Fu G H, Chandra A. The relationship between wafer surface pressure and wafer backside loading in chemical mechanical polishing. *Thin Solid Films* **474**(1–2): 217–221 (2005)
- [42] Wang T, Lu X, Zhao D, He Y. Contact stress non-uniformity of wafer surface for multi-zone chemical mechanical polishing process. *Science China Technological Sciences* **56**(8): 1974–1979 (2013)
- [43] Tseng W T, Wang Y L. Re-examination of pressure and speed dependences of removal rate during chemical-mechanical polishing processes. *J Electrochem Soc* **144**(2): L15–L17 (1997)
- [44] Zhao D W, He Y Y, Wang T Q, Lu X C, Luo J B. Effects of the polishing variables on the wafer-pad interfacial fluid pressure in chemical mechanical polishing of 12-inch wafer. *J Electrochem Soc* **159**(3): H342–H348 (2012)
- [45] Castillo-Mejia D, Beaudoin S. A locally relevant prestonian model for wafer polishing. *J Electrochem Soc* **150**(2): G96–G102 (2003)
- [46] Seok J, Sukam C P, Kim A T, Tichy J A, Cale T S. Multiscale material removal modeling of chemical mechanical polishing. *Wear* **254**(3–4): 307–320 (2003)
- [47] Seok K J, Kim A T, Sukam C P, Jindal A, Tichy J A, Gutmann R J, Cale T S. Inverse analysis of material removal data using a multiscale CMP model. *Microelectron Eng* **70**(2–4): 478–488 (2003)
- [48] Zhao Y W, Chang L. A micro-contact and wear model for chemical-mechanical polishing of silicon wafers. *Wear* **252**(3–4): 220–226 (2002)
- [49] Zhao Y W, Maietta D M, Chang L. An asperity microcontact model incorporating the transition from elastic deformation to fully plastic flow. *J Tribol-T ASME* **122**(1): 86–93 (2000)
- [50] Luo J F, Dornfeld D A. Material removal mechanism in chemical mechanical polishing: theory and modeling. *IEEE T Semiconduct M* **14**(2): 112–133 (2001)
- [51] Shi F G, Zhao B. Modeling of chemical-mechanical polishing with soft pads. *Appl Phys A-Mater* **67**(2): 249–252 (1998)
- [52] Wang Y G, Zhao Y W, Gu J. A new nonlinear-micro-contact model for single particle in the chemical-mechanical polishing with soft pad. *J Mater Process Tech* **183**(2–3): 374–379 (2007)
- [53] Yeruva S B. Particle scale modeling of material removal and surface roughness in chemical mechanical polishing. PhD thesis. Florida (USA): University of Florida, 2005.
- [54] Yeruva S B, Park C W, Rabinovich Y I, Moudgil B M. Impact of pad-wafer contact area in chemical mechanical polishing. *J Electrochem Soc* **156**(10): D408–D412 (2009)
- [55] Greenwood J A, Williamson J B P. Contact of nominally flat surfaces. *Proc R Soc Lond A* **295**(1442): 300–319 (1966)
- [56] Jeng Y, Huang P. A material removal rate model considering interfacial micro-contact wear behavior for chemical mechanical polishing. *J Tribol* **127**(1): 190–197 (2005)
- [57] Uneda M, Maeda Y, Ishikawa K, Ichikawa K, Doi T, Yamazaki T, Aida H. Relationships between contact image analysis results for pad surface texture and removal rate in CMP. *J Electrochem Soc* **159**(2): H90–H95 (2012)
- [58] Cho C H, Park S S, Ahn Y. Three-dimensional wafer scale hydrodynamic modeling for chemical mechanical polishing. *Thin Solid Films* **389**(1–2): 254–260 (2001)
- [59] Park S S, Cho C H, Ahn Y. Hydrodynamic analysis of chemical mechanical polishing process. *Tribol Int* **33**(10): 723–730 (2000)
- [60] Zhang C H, Luo J B, Liu J Q, Du Y P. Analysis on contact and flow features in CMP process. *Chinese Sci Bull* **51**(18): 2281–2286 (2006)
- [61] Sundararajan S, Thakurta D G, Schwendeman D W, Murarka S P, Gill W N. Two-dimensional wafer-scale chemical mechanical planarization models based on lubrication theory and mass transport. *J Electrochem Soc* **146**(2): 761–766 (1999)
- [62] Kim T, Cho Y. Average flow model with elastic deformation for CMP. *Tribol Int* **39**(11): 1388–1394 (2006)
- [63] Ng S H. Measurement and modeling of fluid pressures in chemical mechanical polishing. PhD thesis. Atlanta (USA): Georgia Institute of Technology, 2005.
- [64] Jeng Y, Huang P, Pan W. Tribological analysis of CMP with partial asperity contact. *J Electrochem Soc* **150**(10): G630–G637 (2003)
- [65] Tichy J. Contact mechanics and lubrication hydrodynamics of chemical mechanical polishing. *J Electrochem Soc* **146**(4): 1523–1528 (1999)
- [66] Tsai H J, Jeng Y R, Huang P Y. An improved model considering elastic-plastic contact and partial hydrodynamic lubrication for chemical mechanical polishing. *P I Mech Eng J-J Eng* **222**(J6): 761–770 (2008)
- [67] Hu I, Yang T S, Chen K S. Synergetic effects of wafer rigidity and retaining-ring parameters on contact stress uniformity in chemical mechanical planarization. *Int J Adv Manuf Tech* **56**(5–8): 523–538 (2011)
- [68] Chen R L, Jiang R R, Lei H, Liang M. Material removal mechanism during porous silica cluster impact on crystal silicon substrate studied by molecular dynamics simulation.

- Appl Surf Sci* **264**: 148–156 (2013)
- [69] Chen R L, Liang M, Luo J B, Lei H, Guo D, Hu X. Comparison of surface damage under the dry and wet impact: molecular dynamics simulation. *Appl Surf Sci* **258**(5): 1756–1761 (2011)
- [70] Chen R L, Luo J B, Guo D, Lei H. Dynamic phase transformation of crystalline silicon under the dry and wet impact studied by molecular dynamics simulation. *J Appl Phys* **108**: 0735217 (2010)
- [71] Chen R L, Luo J B, Guo D, Lu X C. Extrusion formation mechanism on silicon surface under the silica cluster impact studied by molecular dynamics simulation. *J Appl Phys* **104**: 10490710 (2008)
- [72] Si L N, Guo D, Luo J B, Lu X C. Monoatomic layer removal mechanism in chemical mechanical polishing process: a molecular dynamics study. *J Appl Phys* **107**: 0643106 (2010)
- [73] Si L N, Guo D, Luo J B, Lu X C, Xie G X. Abrasive rolling effects on material removal and surface finish in chemical mechanical polishing analyzed by molecular dynamics simulation. *J Appl Phys* **109**: 0843358 (2011)
- [74] Si L N, Guo D, Luo J B, Xie G X. Planarization process of single crystalline silicon asperity under abrasive rolling effect studied by molecular dynamics simulation. *Appl Phys A-Mater* **109**(1): 119–126 (2012)
- [75] Han X S, Hu Y Z, Yu S Y. Investigation of material removal mechanism of silicon wafer in the chemical mechanical polishing process using molecular dynamics simulation method. *Appl Phys A-Mater* **95**(3): 899–905 (2009)
- [76] Chen K, Wang Y L. Study of non-preston phenomena induced from the passivated additives in copper CMP. *J Electrochem Soc* **154**(1): H41–H47 (2007)
- [77] Qin K, Moudgil B, Park C W. A chemical mechanical polishing model incorporating both the chemical and mechanical effects. *Thin Solid Films* **446**(2): 277–286 (2004)
- [78] Li J, Liu Y H, Lu X C, Luo J B, Dai Y J. Material removal mechanism of copper CMP from a chemical-mechanical synergy perspective. *Tribol Lett* **49**(1): 11–19 (2013)
- [79] Li J, Lu X C, He Y Y, Luo J B. Modeling the chemical-mechanical synergy during copper CMP. *J Electrochem Soc* **158**(2): H197–H202 (2011)
- [80] Yu J X, Kim S H, Yu B J, Qian L M, Zhou Z R. Role of tribochemistry in nanowear of single-crystalline silicon. *ACS Appl Mater Interfaces* **4**(3): 1585–1593 (2012)
- [81] Liao C L, Guo D, Wen S Z, Luo J B. Effects of chemical additives of CMP slurry on surface mechanical characteristics and material removal of copper. *Tribol Lett* **45**(2): 309–317 (2012)
- [82] Luo J F, Dornfeld D A. Material removal regions in chemical mechanical planarization for submicron integrated circuit fabrication: coupling effects of slurry chemicals, abrasive size distribution, and wafer-pad contact area. *IEEE T Semiconduct M* **16**(1): 45–56 (2003)
- [83] Mueller N, Rogers C, Manno V P, White R, Moinpour M. *In situ* investigation of slurry flow fields during CMP. *J Electrochem Soc* **156**(12): H908–H912 (2009)
- [84] Levert J A, Mess F M, Salant R F, Danyluk S, Baker A R. Mechanisms of chemical-mechanical polishing of SiO_2 dielectric on integrated circuits. *Tribol T* **41**(4): 593–599 (1998)
- [85] Levert J A, Danyluk S, Tichy J. Mechanism for subambient interfacial pressures while polishing with liquids. *J Tribol* **122**(2): 450–457 (2000)
- [86] Shan L, Levert J, Meade L, Tichy J, Danyluk S. Interfacial fluid mechanics and pressure prediction in chemical mechanical polishing. *J Tribol-T ASME* **122**(3): 539–543 (2000)
- [87] Ng S H, Yoon I, Higgs C F, Danyluk S. Wafer-bending measurements in CMP. *J Electrochem Soc* **151**(12): G819–G823 (2004)
- [88] Ng S H, Borucki L, Higgs C F, Yoon I, Osorno A, Danyluk S. Tilt and interfacial fluid pressure measurements of a disk sliding on a polymeric pad. *J Tribol-T ASME* **127**(1): 198–205 (2005)
- [89] Scarfo A M, Manno V P, Rogers C B, Anjur S P, Moinpour M. *In situ* measurement of pressure and friction during CMP of contoured wafers. *J Electrochem Soc* **152**(6): G477–G481 (2005)
- [90] Zhao D W, He Y Y, Lu X C. *In situ* measurement of fluid pressure at the wafer-pad interface during chemical mechanical polishing of 12-inch wafer. *J Electrochem Soc* **159**(1): H22–H28 (2011)
- [91] Zhao D W, He Y Y, Wang T Q, Lu X C, Luo J B. Wafer bending/orientation characterization and their effects on fluid lubrication during chemical mechanical polishing. *Tribol Int* **66**: 330–336 (2013)
- [92] Zhao D W, Wang T Q, He Y Y, Lu X C. Effect of zone pressure on wafer bending and fluid lubrication behavior during multi-zone CMP process. *Microelectron Eng* **108**: 33–38 (2013)
- [93] Li J, Liu Y, Dai Y, Yue D, Lu X, Luo J. Achievement of a near-perfect smooth silicon surface. *Science China Technological Sciences* **56**(11): 2847–2853 (2013)



Xinchun LU. He received the BS and MS degrees in material science and engineering from Jilin University of Technology, Changchun, China, in 1988 and 1991, respectively, and the PhD degree in the same field from the Institute of Metal Research, Chinese Academy of Sciences, in 1994.

He is a chair professor of Changjiang Scholars in the Department of Precision Instruments and Mechanology of Tsinghua University, China, and is a member of the international executive committee of ICPT. His current areas of research include micro-nano fabrication technology, the theory and applications of the

micro-nano tribology of the surface and interface, and equipment and processes of chemical mechanical polishing. He is the author or coauthor of over 100 journal publications and conference proceedings papers. He holds over 16 patents in the area of CMP equipment.

Prof. Lu was the recipient of the Trans-Century Training Program of the National Ministry of Education, and the National Science Found for Distinguished Young Scholars of China. He has received numerous national awards, including the Award for National Science Development (grade two), and the Science & Technology Advancement Award (grade one), from the National Ministry of Education.



Dewen ZHAO. He received the BS degree in mechanical engineering from Huazhong University of Science and Technology, Wuhan, China, in 2007, and the PhD degree in mechanical engineering from Tsinghua University, Beijing, China in 2012.

He received the Bronze Medal of HIWIN Doctoral

Dissertation Award in 2013. Dr. Zhao is currently a postdoctoral research fellow at Tsinghua University, Beijing, China. He has more than 10 papers indexed by SCI, and 9 authorized national invention patents. His major research areas include chemical mechanical polishing equipment and principles, tribology, and process monitoring.

